

Fluctuation-Induced Momentum Transport and Plasma Flow in the MST Reversed Field Pinch

D.L. Brower 1), W.X. Ding 1), L. Lin 1), W.F. Bergerson 1), A.F. Almagri 2), D.J. Den Hartog 2), G. Fiksel 3), V.V. Mirnon 2), J.A. Reusch 2), J.S. Sarff 2)

1) University of California, Los Angeles, California 90095 USA

2) University of Wisconsin-Madison, Madison, Wisconsin 53706 USA

3) Laboratory for Laser Energetics, University Rochester, New York 14623 USA

e-mail: brower@ucla.edu

Abstract: For the first time, the fluctuation-induced momentum flux in a stochastic magnetic field has been directly measured in the core of a high-temperature, magnetically-confined, toroidal plasma. Parallel pressure fluctuations play an important role in momentum transport with the magnetic fluctuation-induced momentum flux arising from the correlated product of density and radial magnetic field fluctuations. The measured momentum flux can largely account for changes in plasma flow and momentum redistribution during a magnetic reconnection event. The origin of the momentum flux surge at the sawtooth crash is related to nonlinear interactions that alter the phase relation between density and magnetic fluctuations so as to maximize transport.

1. Introduction

Fluctuations have long been considered a likely candidate for explaining energy, particle, and momentum transport in various toroidal magnetic confinement configurations. In particular, the physics of intrinsic plasma rotation, flow change associated with resonant magnetic perturbations, and momentum transport is of great importance to fusion plasma research as flows can act to improve or degrade performance. Plasmas in the Madison Symmetric Torus (MST) reversed-field pinch (RFP) rotate spontaneously and this rotation abruptly changes during repetitive bursts of current-driven resistive tearing instabilities that stochastize the magnetic field and cause reconnection (sawtooth crash). In this paper, we report the first measurements of magnetic fluctuation-induced momentum flux in the core of the MST RFP, particularly during the sawtooth crash when the stochastic fields are strongest. Direct measurements of the stochastic field driven momentum flux are made using a high-speed, laser-based, interferometer and Faraday rotation system. Measurements show (1) ion momentum flux from stochastic magnetic field can account for the equilibrium flow change during reconnection, and (2) multiple, global reconnections are required for momentum transport. When only the core resonant modes are excited and the edge modes remain small, the change in the plasma rotation and magnetic fluctuation-induced flux are largely eliminated. Momentum flux arises from finite radial magnetic field correlation with parallel pressure fluctuations caused by density perturbations. The origin of these density fluctuations is identified and related to nonlinear three-wave interactions.

2. Experimental Results

Magnetic reconnection is characterized by discrete sawtooth-like bursts in both tokamaks and RFPs. For typical MST plasmas without current profile control, plasma ion flow relaxation (i.e., decrease in core flow and increase in edge flow), as shown in Fig. 1, occurs much faster (<200 μ sec) than can be explained by classical collision processes (\sim 10 msec). Data are

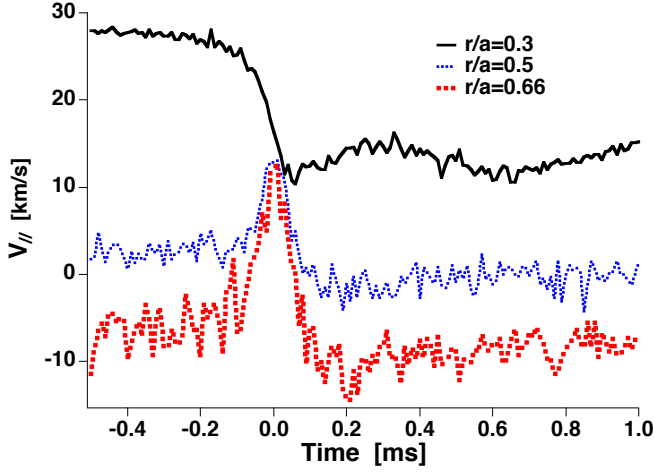


Figure 1. Plasma parallel flow during the sawtooth cycle at three radial locations in MST.

to the parallel Maxwell stress, when evaluated for the plasma ions is observed to be much larger and opposite in sign to the inertial term, $\rho_i \partial < V_{\parallel,i} > / \partial t$, in the fluid ion momentum equation, as shown in Fig. 2, where $\rho_i = M_i n$ is the ion mass density and $\partial < \rho_i V_{\parallel,i} > / \partial t = \rho_i \partial < V_{\parallel,i} > / \partial t + V_{\parallel,i} \partial < \rho_i > / \partial t$. Measurements in the edge region of MST plasmas indicate the large Maxwell stress is offset by the Reynolds stress, which is of comparable amplitude but opposite sign [2]. The Reynolds stress has not been measured in the plasma core.

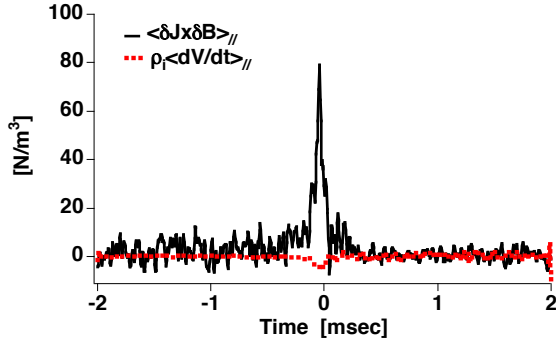


Figure 2. EM torque and inertial terms from fluid ion momentum equation.

Momentum flux can also arise from finite parallel pressure fluctuations in a stochastic magnetic field [3], *i.e.*, $\Gamma_{r,ion} = \langle \delta p_{\parallel,i} \delta b_r \rangle / B$, where $\langle \dots \rangle$ represents a flux surface average and the parallel fluctuating ion pressure can be divided into two components $\delta p_{\parallel,i} = T_{\parallel,i} \delta n + n \delta T_{\parallel,i}$. Consequently, the magnetic fluctuation-induced momentum flux can be rewritten as the sum of two terms

$$\Gamma_{r,ion} = \frac{\langle \delta p_{\parallel,i} \delta b_r \rangle}{B} = T_{\parallel,i} \frac{\langle \delta n \delta b_r \rangle}{B} + n \frac{\langle \delta T_{\parallel,i} \delta b_r \rangle}{B} . \quad (1)$$

The first term, corresponding to the correlated product of radial magnetic field and density fluctuations, is referred to as the density term. The second term, which goes as the correlated product of radial magnetic field and parallel ion temperature fluctuations, is labeled the temperature term. Balancing parallel momentum change with the radial momentum flux leads to

$$\rho_i \frac{\partial V_{\parallel,i}}{\partial t} = -\nabla \left(\frac{\langle \delta p_{\parallel,i} \delta b_r \rangle}{B} \right) \approx -\nabla \left(\frac{T_{\parallel,i}}{B} \langle \delta n \delta b_r \rangle \right) - \nabla \left(\frac{n}{B} \langle \delta T_{\parallel,i} \delta b_r \rangle \right) . \quad (2)$$

ensembled over the sawtooth cycle with $t=0$ denoting crash. Similar relaxation for the current density distribution is observed at the sawtooth crash [1]. Balance in the electron momentum equation (i.e., generalized Ohm's law) is achieved at the crash by including the 2-fluid Hall dynamo effect. The Hall electromotive force is found to be significant ($\langle \delta \mathbf{J} \times \delta \mathbf{B} \rangle_{\parallel} / n_e e \sim 40$ V/m), suppressing (flattening) the equilibrium core current near the mode resonant surface. However, this same electromagnetic torque, $\langle \delta \mathbf{J} \times \delta \mathbf{B} \rangle_{\parallel}$ which is equivalent

Measurement comparison between the divergence of momentum flux and the inertial term, $\rho_i \partial V_{||,i} / \partial t$, has been made in the core of MST plasmas.

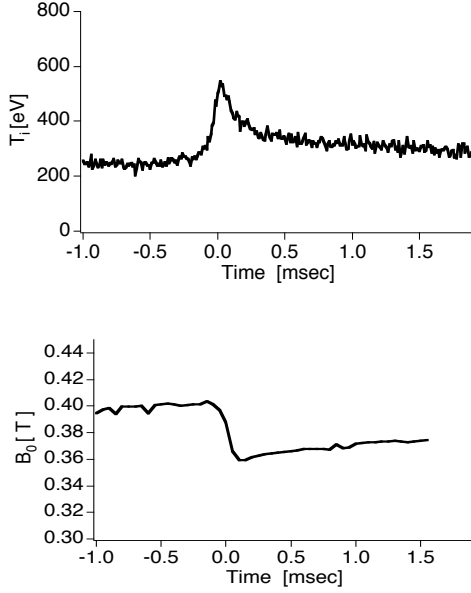


Figure 3. (a) Parallel ion temperature and (b) axial magnetic field evolution during the sawtooth cycle. Time $t=0$ denotes crash.

To quantitatively investigate the effect of magnetic field fluctuations on momentum transport and flow relaxation, we must measure both the magnetic fluctuation-induced flux and its divergence. We focus first on the measurement of the core fluctuation-induced momentum flux density term and its derivative which requires measurement of (1) equilibrium parallel ion temperature and axial magnetic field, (2) local density fluctuations and their derivative, δn , $\partial \delta n / \partial r$, (3) magnetic field fluctuation δb_r , and (4) their correlation, $\langle \delta n \delta b_r \rangle$. This is accomplished on MST using multiple diagnostics. Bulk (impurity) ion flow and temperature is measured by Rutherford scattering (CHERS) while the axial toroidal magnetic field is determined from MSE. The fluctuating density and magnetic field in the plasma core are measured using a combined laser-based polarimeter (Faraday effect) - interferometer diagnostic with high temporal (~ 1 msec) and phase resolution (1 mrad at 50

kHz bandwidth). The 11 vertically-viewing chords (separation ~ 8 cm) provide information on the amplitude, spatial distribution and phase for modes of specified helicity [2,4]. Both the equilibrium and fluctuating density gradient are obtained using conventional and differential interferometry techniques [5,6].

In cylindrical coordinates, the expression for gradient of the flux, Eq.(2), can be simplified since measurements show that the parallel ion temperature, mean magnetic field, and radial magnetic field fluctuation profiles are nearly flat in the core [1,7]. Therefore, we can write $\nabla \left(\frac{T_{||,i} \langle \delta n \delta b_r \rangle}{B} \right) \approx 2 \frac{T_{||,i}}{B} \langle \frac{\partial \delta n}{\partial r} \delta b_r \rangle$. In the following, measurement of each quantity, equilibrium and fluctuating, will be described.

Measurements reported herein were carried out on the MST RFP with major radius $R_0=1.5$ m, minor radius $a=0.52$ m, discharge current 350~400 kA, line-averaged electron density $\bar{n}_e \sim 1 \times 10^{19} m^{-3}$, and temperature $T_e \sim T_i \sim 400 eV$ for a deuterium plasma. Ion parallel temperature is observed to more than double at the sawtooth crash, from 250 to 550 eV while the axial magnetic field is reduced by $\sim 10\%$, as shown in Fig. 3.

In general, density fluctuations can be written as $\delta n = \sum \delta n_{m,n} \cos(m\theta + n\phi + \Delta(r))$ where m, n, Δ are the poloidal and toroidal mode numbers and phase, respectively. In MST, the dominant modes are $m=1$ and the fluctuating interferometric phase is given by $\delta \phi(x) = c_1 \int \delta n_{m=1}(r) \cos(\theta) dz$, where $c_1 = 1.20 \times 10^{-18} m^2$ for laser wavelength 432 μm . The term $\cos \theta = x/r$, where x is the impact parameter, is a geometrical weighting factor which

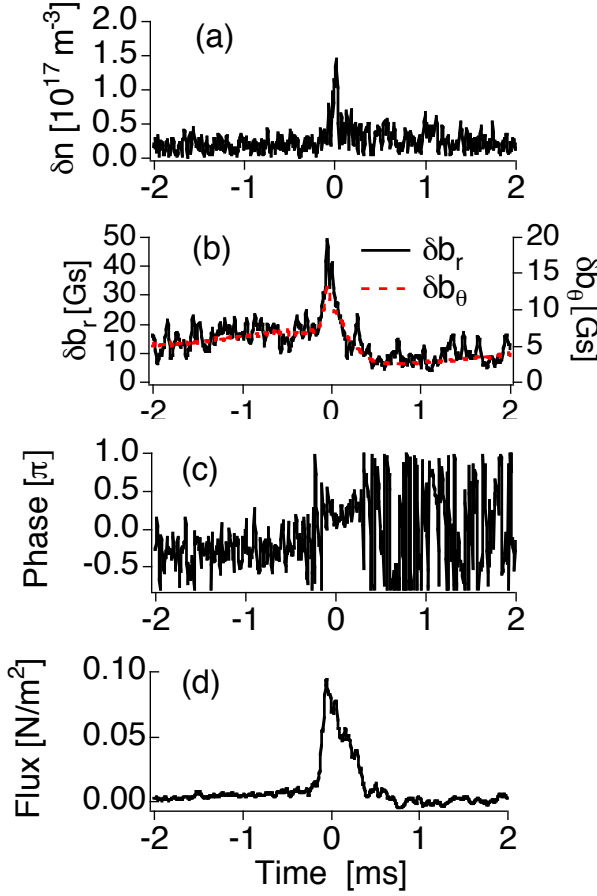


Figure 4. Measurements of (a) density and (b) magnetic fluctuations, (c) their phase relation, and (d) momentum flux at $r/a \sim 0.1$ for the $(m,n)=(1,6)$ mode.

approaches a delta function as $x \rightarrow 0$ thereby providing spatial resolution of ~ 10 cm in the plasma core. This leads to a simple relation between phase fluctuations and density fluctuations for chords close to the plasma center, *i.e.* $\delta n(r) \approx \delta \phi(x)/2ac_1$. The fluctuating line-integrated phase is equivalent to the local density fluctuation amplitude. The radial magnetic field fluctuations in the core are obtained by Faraday rotation measurement. Previously, it has been established that radial magnetic fluctuations dominate Faraday rotation fluctuations ($\delta\Psi$) for chords close to the magnetic axis [4,5,6], leading to $\delta\Psi \sim \int n_e \delta b_r dz$. Hence the Faraday measurement can be used to provide a direct line-integrated measure of δb_r .

The measured density and magnetic field fluctuations exhibit a significant surge at the sawtooth crash as shown in Figs. 4 (a) and (b), respectively. Density fluctuations away from the sawtooth crash are approximately 0.15%, reaching 1% at the crash. This is qualitatively consistent with the observation that the largest flow change occurs at the sawtooth crash, suggesting that large density fluctuations contribute

to flow relaxation. Maximum magnetic fluctuation amplitude also occurs at the crash where the δb_r increases by a factor of 3. For comparison, the poloidal magnetic fluctuation amplitude (dashed line) measured at the wall is also plotted. The local radial magnetic fluctuation profile is obtained by numerically fitting experimental data as described in earlier work [5,6]. The radial magnetic field fluctuation amplitude (1-2% at crash) in the core is approximately three times the poloidal magnetic field at the wall, *i.e.* $\delta b_r(0) \sim 3 \times \delta b_\theta(a)$, consistent with the results from MHD computation. These data are for fluctuations at $r/a=0.10$ associated with the dominant core tearing mode ($m=1, n=6$) obtained by cross correlation with the specific helical magnetic mode obtained from spatial Fourier decomposition of measurements from an array of 32 wall-mounted magnetic coils at the plasma surface. Finally, the correlated product between δn (or $\partial \delta n / \partial r$) and δb_r is obtained by ensemble averaging. In MST, rotation of the low- n magnetic modes transfers their spatial structure in the plasma frame into a temporal evolution in the laboratory frame. Since the magnetic modes are global, for convenience we correlate δn (or $\partial \delta n / \partial r$) with a specific helical magnetic mode obtained from the spatial Fourier decomposition noted above. After averaging over an ensemble of ~ 400 similar events, we determine the correlated product between δn (or $\partial \delta n / \partial r$) and δb_r for all modes. With combined measurements of density fluctuations, radial magnetic fluctuations and their correlated product, the magnetic

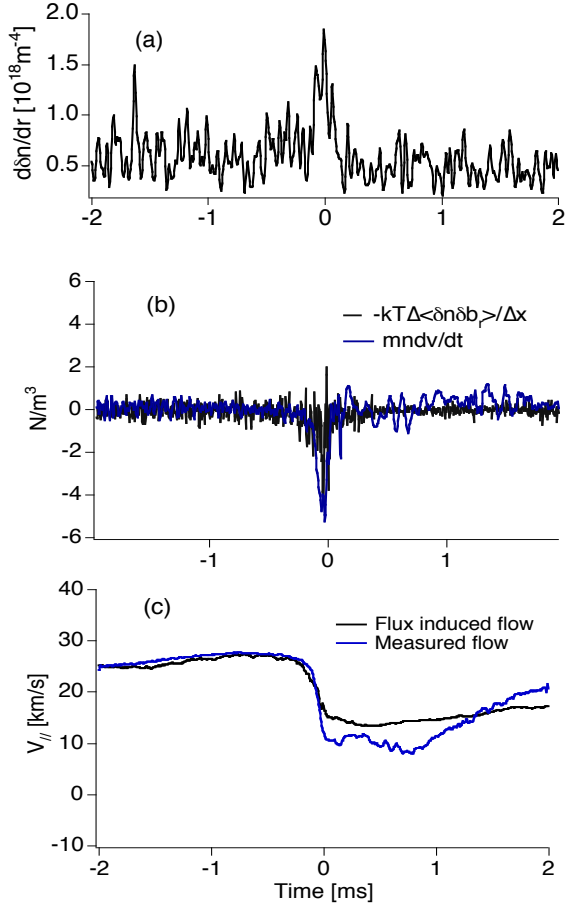


Figure 5. (a) density fluctuation gradient, (b) divergence of fluctuation-induced momentum flux at $r/a=0.1$ (solid black line). Solid blue line is the $\rho_i \partial \langle V_{\parallel,i} \rangle / \partial t$ inertial term (c) Time integrated flux divergence (solid line) and ion parallel flow (dashed line). Flow at $t=-0.5$ ms is taken as an integral constant.

flow at $t=-0.5$ ms is taken as an integral constant.

While the measured core fluctuation-induced momentum transport is significant and can largely account for the observed core flow relaxation, the divergence of the fluctuation-induced momentum flux associated with ion temperature, $\sim \nabla \langle \delta T_{\parallel,i} \delta b_r \rangle$, is not measured and may also contribute to the total flux. However, when calculating the momentum flux summed over all modes $m=1, n=6-15$, better agreement is obtained with $\rho_i \partial V_{\parallel,i} / \partial t$, implying contributions from the $\nabla \langle \delta T_{\parallel,i} \delta b_r \rangle$ term are smaller. The $V_{\parallel,i} \partial \langle \rho_i \rangle / \partial t$ term, which is $\sim 30\%$ of the $\rho_i \partial \langle V_{\parallel,i} \rangle / \partial t$ term, as shown in Fig. 6, is offset by the magnetic fluctuation-induced particle flux [8].

Evaluation of the magnetic fluctuation-induced momentum flux (density term) towards the plasma edge, $r/a \sim 0.5$, can also be made and is shown in Fig. 7. Here, contributions from the gradient of δb_r have been included. Like the core measurement, at half the minor radius the momentum flux also surges but has opposite sign. The time integrated momentum flux now

fluctuation-induced momentum flux (density term) can be determined as shown in Fig. 4(d). Contributions from the largest modes ($m=1, n=6,7,8,9$) have been summed. At the sawtooth crash, δn and δb_r are nearly in phase [see Fig. 4(c)] as the momentum flux surges to ~ 0.1 N/m², concurrent with the core flow relaxation shown earlier in Fig. 1.

In order to relate this measured fluctuation-induced momentum flux to changes in plasma flow, we need to compare the gradient of the flux with the time derivative of the flow, $\nabla \left(\frac{T_{\parallel,i} \langle \delta n \delta b_r \rangle}{B} \right)$ and $\rho_i \partial \langle V_{\parallel,i} \rangle / \partial t$. This

requires measurements of the density fluctuation gradient, which is shown in Fig. 5(a). Like the density fluctuations, the gradient also exhibits a surge at the crash. Fast flow profile relaxation (see Fig.1) implies a surge of $dV_{\parallel,i} / dt$, as indicated in Fig. 5(b). The measured flux divergence ($\nabla \cdot \Gamma_{r,i}^{\delta n}$) shows a similar increase, essentially balancing the parallel flow change within experimental errors. One can integrate these traces over time to directly compare the flow change and momentum flux flow as shown in Fig. 5(c). Here we see that magnetic field driven momentum flux arising from density fluctuations, matches the observed core parallel flow decrease at a sawtooth crash, both in amplitude and temporal evolution.

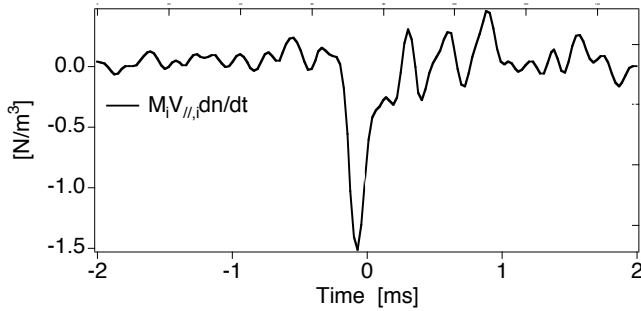


Figure 6. $V_{||,i} \partial \langle \rho_i \rangle / \partial t$ term during sawtooth cycle.

magnetic field fluctuations for a contributing mode must differ from $\pi/2$. In MST, we observe that the phase deviates significantly from $\pi/2$ only when three-wave coupling is strong. That is, it appears that the phase between density and magnetic field fluctuations for a specific mode is altered if that mode is nonlinearly coupled to other modes, and the alteration is such as to increase the momentum flux. We draw this conclusion by comparing the fluctuation-induced momentum flux in standard RFP plasmas to plasmas in which the dominant three-wave interactions are eliminated. This effect of nonlinear mode coupling is similar to recent results from MHD computation [9].

Experimentally observed phase deviation from $\pi/2$ [see Fig. 4(c)] during a sawtooth crash

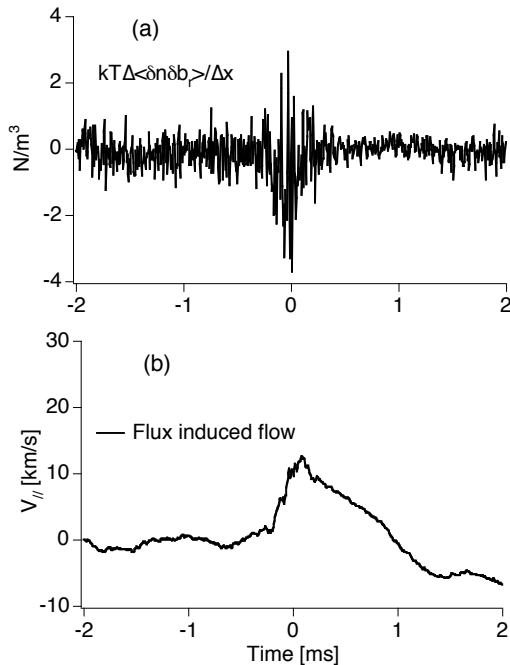


Figure 7. (a) Divergence of magnetic fluctuation-induced momentum flux at $r/a=0.5$ (b) Flow from time-integrated flux divergence. Flow at $t=-0.5$ ms is taken as an integral constant. Time $t=0$ denotes sawtooth crash.

shows an increased flow at the crash, as opposed to a decrease at the magnetic axis as shown in Fig. 5(c). This observation is qualitatively consistent with the increased flow shown in Fig. 1, for this region of the plasma, and implies momentum transport from core toward the edge as opposed to total momentum loss at the crash.

For the fluctuation-induced momentum flux to be nonzero, the phase between density and radial

implies that the momentum flux is enhanced. The phase change most likely originates from nonlinear mode coupling in MST plasmas since magnetic fluctuations can interact with the eddy currents generated by global magnetic field perturbations, similar to the effect of an error field [10] or imposed boundary [11]. The measured safety factor at the magnetic axis is $q(0) \sim 0.2$, and monotonically decreasing at larger minor radii. It passes through zero at the reversal surface, being negative at the edge, as shown in Fig. 8. From the measured q profile, resonant low- n ($n=6$ is the resonant mode closest to the magnetic axis), $m=1$ magnetic modes will dominate the core magnetic fluctuation wave number spectrum as is frequently observed. In addition to the core resonant modes, $m=0$ ($n=1, 2, \dots$) modes are resonant at the reversal surface ($q=0$) close to the boundary. Both the $m=1$ and $m=0$ tearing modes have a global nature so that nonlinear mode coupling is common [12,13]. The 3-wave interaction has to satisfy the sum rule

$$m_1 \pm m_2 = m_3 \quad \text{and} \quad n_1 \pm n_2 = n_3. \quad (3)$$

The coupling of two adjacent $m=1$ modes via interaction with an $m=0$ mode has been shown to be very important in both experiments and MHD computation.

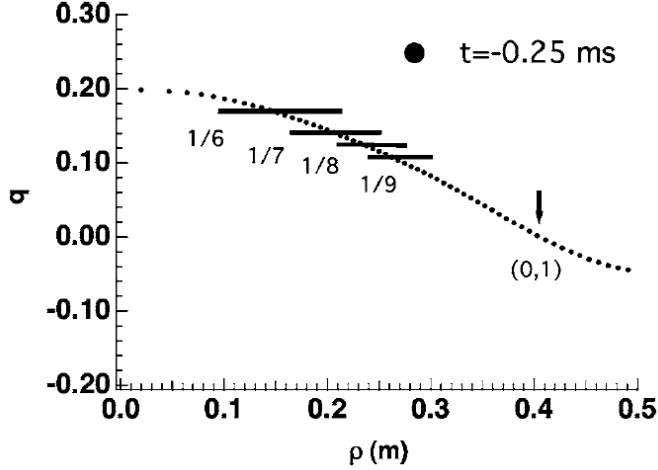


Figure 8. The safety factor q profile 0.25 ms before sawtooth crash. The $m=1$ resonant surfaces and island width are indicated by solid line and the $m=0$ surface by arrow. Solid circles represent the measured q profile. Mode resonant surfaces are densely packed resulting in strong mode-mode interaction.

plasmas. However, the $m=0$ mode amplitude is significantly reduced, as shown in Fig. 9, since its resonant surface is removed. For non-reversed plasmas, measurements reveal the

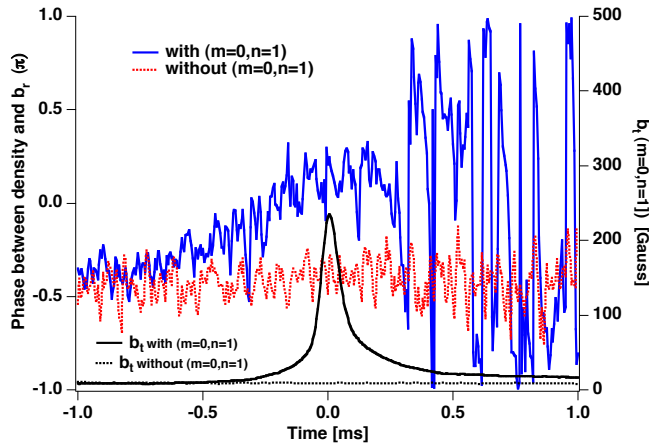


Figure 9. $\langle \delta n \delta b_r \rangle$ phase ($m=1, n=6$) and δb_{tor} ($m=0, n=1$) for reversed [with (0,1) surface] and non-reversed [without (0,1) surface] RFP plasmas.

A typical strong three wave interaction observed in MST plasmas is that between the (1,6), (1,7) and (0,1) modes. The suppression of one mode is expected to result in a dramatic reduction in the nonlinear mode coupling. In order to identify the role played by nonlinear coupling in the fluctuation-induced momentum flux during the sawtooth crash, we compare standard RFP plasmas with those where the reversal surface (i.e., $q=0$ resonance surface) has been removed (i.e., non-reversed MST plasmas where the reversal surface is moved beyond or located at $r=a$). For reversed plasmas, the $m=1, n=6, 7, 8, \dots$ mode amplitudes during the sawtooth cycle are found to be comparable to the non-reversed case. This indicates that the $m=1$ mode does not decrease significantly for non-reversed

plasmas. However, the $m=0$ mode amplitude is significantly reduced, as shown in Fig. 9, since its resonant surface is removed. For non-reversed plasmas, measurements reveal the fluctuation-induced momentum flux is reduced 10-fold compared to standard RFP plasmas and is observed to peak at $\sim 0.01 \text{ N/m}^3$, as shown in Fig. 10(a). The phase between the localized density fluctuations and global radial magnetic fluctuation for the (1,6) mode is also altered as shown in Fig. 9. From these results it is apparent that to have the phase differ significantly from 90 degrees, substantial $m=0$ activity is needed, implying that the change in (1,6) mode phase between δn and δb_r occurs due to nonlinear coupling. That the measured fluctuation-induced momentum flux is responsible for the change in the

plasma flow is also clarified by these experiments. As shown in Figs. 10(b) and (c), when the nonlinear coupling is absent and the fluctuation-induced momentum flux is reduced 10-fold,

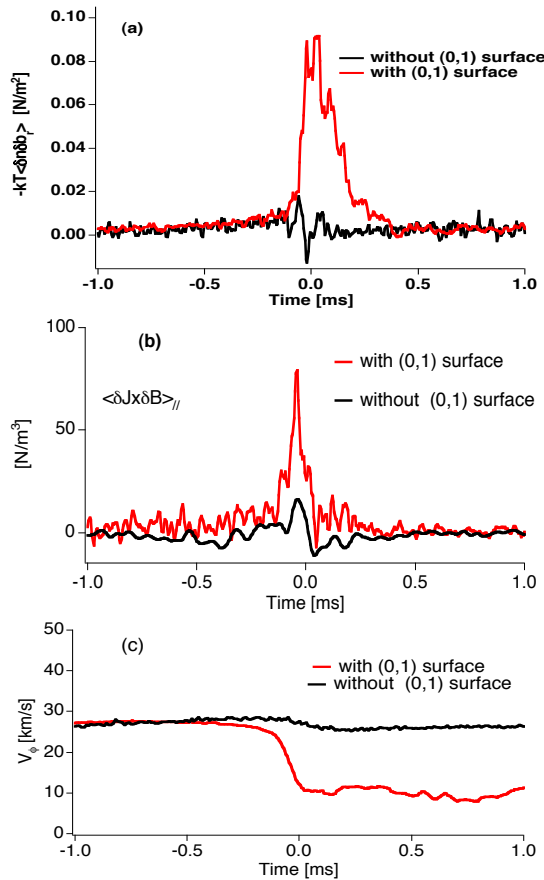


Figure 10. (a) Fluctuation-induced momentum flux, (b) $\langle \delta \vec{J} \times \delta \vec{B} \rangle_{\parallel}$ ion torque and (c) core plasma flow during sawtooth cycle. Red traces corresponds to standard RFP plasmas while black traces refer to plasmas with no (0,1) resonant surface.

the electromagnetic torque on plasma ions and plasma flow change is reduced by a comparable amount.

3. Summary

In summary, a direct measurement of magnetic fluctuation-induced momentum flux and its divergence has been made, for the first time, in the core of a high-temperature plasma. The surge in fluctuation-induced momentum flux during a sawtooth crash is consistent with changes in plasma parallel flow and momentum relaxation. Overall, it is clear that pressure fluctuations play an important role in momentum transport with the fluctuation-induced momentum flux largely arising from the correlated product of density and radial magnetic field fluctuations. Experiments demonstrate that nonlinear mode-mode coupling is an essential ingredient to generating significant momentum flux. Nonlinear mode coupling alters the phase relation between the density and radial magnetic field fluctuations with large phase deviation from $\pi/2$ occurring only when three wave coupling is strong.

References

- [1] W.X.Ding, *et al.*, Phys. Rev. Lett. **93**, 045002(2004).
- [2] A. Kuritsyn, *et al.*, Physics of Plasmas **16**,055903(2009).
- [3] S.C. Prager, *et al.*, PPCF, Vol.41, A129(1999).
- [4] W.X. Ding, *et al.*, Phys. Rev. Lett. **90**, 035002(2003).
- [5] W.X. Ding, D.L. Brower and T.Y. Yates, Rev. Sci. Instrum. **79**,10E701 (2008); W.X. Ding, D.L. Brower, B.H. Deng and T. Yates, Rev. Sci. Instrum. **77**,10F105 (2006).
- [6] W.X. Ding, D.L. Brower and T.Y. Yates, Rev. Sci. Instrum. **79**,10E701 (2008).
- [7] W.X. Ding, *et al.*, Physics of Plasmas **13**, 112306(2006).
- [8] W.X. Ding, D.L. Brower, *et al.*, Phys. Rev. Lett. **103**, 025001(2009).
- [9] S. Ortolani and D. D. Schnack, *Magnetohydrodynamics of Plasma Relaxation*, World Scientific, Singapore, 1993.
- [10] R. Fitzpatrick, Nuclear Fusion **33**, 1049(1993).
- [11] X.G. Wang, Z.W. Ma and A.Bhattacharijee, Physics of Plasmas, **3**,2129 (1996); Z.W. Ma, X.G.Wang and A. Bhattacharjee, Physics of Plasmas, **3**,2427 (1996).
- [12] A.K. Hansen, *et al.*, Phys. Rev. Lett. **85**, 3408(2000).
- [13] T. Bolzonella, D. Terranova, Plasma Physics and Controlled Fusion, **44**, 2569(2002).